Journal of Crystal Growth 323 (2011) 127–131

Contents lists available at ScienceDirect

Journal of Crystal Growth

journal homepage: www.elsevier.com/locate/jcrysgro

Growth and material properties of ZnTe on GaAs, InP, InAs and GaSb (0 0 1) substrates for electronic and optoelectronic device applications

J. Fan [a,b], L. Ouyang [a,b], X. Liu [c], D. Ding [a,d], J.K. Furdyna [c], D.J. Smith [a,b], Y.-H. Zhang [a,d,*]

[a] Center for Photonics Innovation, Arizona State University, Tempe, AZ 85287, USA
[b] Department of Physics, Arizona State University, Tempe, AZ 85287, USA
[c] Department of Physics, University of Notre Dame, Notre Dame, IN 46556, USA
[d] School of Electrical, Computer and Energy Engineering, Arizona State University, Tempe, AZ 85287, USA

ARTICLE INFO

Available online 9 December 2010

Keywords:
A1. X-ray diffraction
A3. Molecular beam epitaxy
B2. Semiconducting II–VI materials
B3. Infrared devices

ABSTRACT

Thick ZnTe grown on III–V substrates is proposed as a low-cost virtual substrate for electronic and optoelectronic device applications based on 6.1 Å compound semiconductors. This paper reports the growth of ZnTe samples on GaAs, InP, InAs and GaSb (0 0 1) substrates using molecular beam epitaxy (MBE). X-ray diffraction (XRD) and high-resolution electron microscopy (HREM) are used to characterize the structural properties, and photoluminescence (PL) is used to characterize the optical properties. XRD analysis indicates there are residual tensile strains in ZnTe epilayers due to the difference in thermal expansion coefficients between the ZnTe epilayers and the different substrate materials. HREM images reveal the presence of Lomer edge and 60° partial dislocations at the interfaces between ZnTe epilayers and GaAs and InP substrates. Visible photoluminescence from ZnTe epilayers is observed from 80 to 300 K.

1. Introduction

ZnTe is a direct-band semiconductor with a bandgap of 2.26 eV (549 nm). It is considered to be suitable for various optoelectronic devices such as pure-green light-emitting diodes, green laser diodes, UV-green photodetectors, and multijunction solar cells [1,2]. Although pure-green ZnTe LEDs have been successfully demonstrated on ZnTe substrates [3,4], one of the big obstacles in making them commercially applicable is the high cost and small size of current ZnTe bulk substrates. It is therefore highly desirable to have larger wafer size ZnTe virtual substrates. Thin ZnTe grown on Si has also been used for ZnCdTe virtual substrates for HgCdTe infrared detectors [5–7]. However, due to the large lattice mismatch between ZnTe and Si, such thin ZnTe layers grown on Si have high misfit dislocation density. Since ZnTe has a lattice constant of 6.1037 Å, which is nearly lattice-matched to 6.1 Å III–V substrates, such as GaSb with a mismatch of only 0.13%, and InAs with a mismatch of 0.75%, ZnTe grown on these substrates is expected to have low density of misfit dislocations. Moreover, GaAs and InP are also good substrate candidates for electronic devices and infrared photo-detectors due to their semi-insulating properties and transparency in the infrared range [8]. Thus, the ability to achieve high quality ZnTe epitaxial growth on these different substrates, and the possibility to reduce the overall material cost, are very important considerations not only for ZnTe related devices, but also for electronic and optoelectronic device applications based on these 6.1 Å compound semiconductors that can be grown lattice matched to ZnTe virtual substrate.

In this paper, we propose the use of thick ZnTe epilayers grown on III–V substrates as low-cost virtual substrates. A set of ZnTe samples has been grown on GaAs, InP, InAs and GaSb (0 0 1) substrates using molecular beam epitaxy (MBE), and the material properties of the ZnTe films have been investigated. During MBE growth, *in situ* reflection high energy electron diffraction (RHEED) is used for growth monitoring and optimization. X-ray diffraction (XRD) measurements are performed to analyze the strain of the ZnTe epilayers and high resolution electron microscopy (HREM) is used to study the structural properties of the ZnTe epilayers, especially misfit dislocations at the interface. Photoluminescence is also applied to characterize the optical properties of the ZnTe epilayers. Growths of high-quality ZnTe samples are successfully demonstrated on all four substrates.

2. Experiments

The epitaxial growth was carried out using an MBE system consisting of III–V and II–VI chambers connected with an ultra-high-vacuum transfer module. The vacuum of the transfer chamber was typically about 5×10^{-9} Torr, which prevented any significant contamination during sample transfer. For growth of the samples, the

* Corresponding author at: School of Electrical, Computer and Energy Engineering, Arizona State University, Tempe, AZ 85287, USA.
Tel.: +1 480 965 2562; fax: +1 480 965 0775.
E-mail address: yhzhang@asu.edu (Y.-H. Zhang).

0022-0248/$ - see front matter © 2010 Elsevier B.V. All rights reserved.
doi:10.1016/j.jcrysgro.2010.11.164

substrates were firstly deoxidized in the III–V chamber, followed by growth of III–V semiconductor buffer layers. The substrate temperatures were measured with a thermocouple on the back of the substrate holder. The growth orientation for all samples was (0 0 1). After the samples were cooled down to room temperature, they were transferred to the II–VI chamber where the ZnTe layers were grown. The substrate temperature during ZnTe growth was 330 °C. The growth parameters for the samples described in this paper are summarized in Table 1.

During growth, the beam equivalent pressure (BEP) ratios of Zn to Te were adjusted to optimize the growth conditions by monitoring the surface reconstructions using RHEED. The RHEED patterns for ZnTe samples appeared to be similar regardless of the specific III–V substrate used for the growths. As an example, RHEED patterns for ZnTe grown on InAs (0 0 1) substrate are shown in Fig. 1. A (2×4) reconstruction of the InAs surface is visible before growth of the ZnTe layer was commenced. At the beginning of ZnTe growth, the RHEED pattern showed a spotty and weakly defined pattern, indicating a transition from the (2×4) to the (1×2) surface reconstruction. The transition time was in the range of 10 s to 1 min. After the transition of the surface reconstruction, the typical ZnTe (1×2) pattern appeared and stayed bright and streaky throughout the rest of the ZnTe growth.

The cross-sectional HREM samples were prepared using mechanical polishing and dimpling followed by ion-beam thinning. Liquid nitrogen and low energy (2.5–3 keV) ion beams were used to avoid any thermal damage. Images were recorded using a JEM-4000EX HREM operated at 400 keV with a structural resolution of ~1.7 Å. The high-resolution XRD rocking curve measurements were performed using a PANalytical X'Pert PRO MRD X-ray diffractometer with multi-crystal monochromator. The copper $K\alpha_1$ line (1.54 Å) was used as the incident beam. For characterization of optical properties, temperature-dependent PL measurements were carried out using the 488 nm line of an Argon ion laser for excitation and a high-resolution grating spectrometer equipped with a photomultiplier for detection.

Table 1
Growth parameters for the ZnTe samples.

Sample no.	Substrate	Zn:Te BEP ratio	Growth rate (nm/s)	Lattice mismatch (%)	ZnTe layer thickness (μm)
I	GaAs	1.2:1	0.30	7.30	2.5
II	InP	1.2:1	0.28	3.85	2.3
III	InAs	1.2:1	0.30	0.75	2.4
IV	GaSb	1.2:1	0.31	0.13	2.5

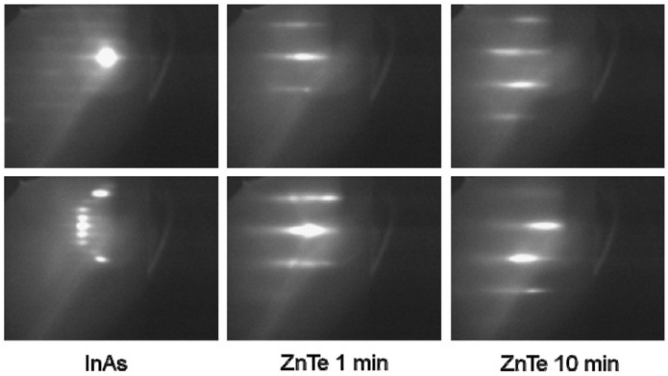

Fig. 1. RHEED patterns recorded during the growth of ZnTe on InAs (0 0 1). The patterns in upper and lower rows are referred to the [1 1 0] and [1$\bar{1}$0] axes, respectively.

3. Results and discussion

After completion of growth, high-resolution XRD measurements are performed on all samples in the vicinity of the (0 0 4) and (3 1 1) diffraction peaks of the substrates. These XRD patterns show two clear diffraction peaks coming from both the ZnTe epilayer and the particular substrate material. Fig. 2 compares the XRD patterns of ZnTe epilayers grown on the various substrates. The full-width at half-maximum (FWHM) of the ZnTe epilayers are in the range of 33–60 arcsec, indicating that the thick ZnTe layers grown on all four substrates are of high quality.

Due to the different lattice constants between ZnTe and the various III–V (0 0 1) substrates, strain occurs in the ZnTe epilayers during growth, making the lattice constants of the ZnTe epilayers different from that of bulk ZnTe. The room temperature lattice constants of ZnTe along the growth direction ($a_\perp$) and in the layer plane ($a_\parallel$) are calculated from the XRD results obtained for the (0 0 4) and (3 1 1) reflections, using Bragg's Law and the following equations

$$a_\perp = \left(\frac{\sin\theta_s}{\sin\theta_{epi}}\right)a_s \tag{1}$$

$$\left(\frac{h}{a_\parallel}\right)^2+\left(\frac{k}{a_\parallel}\right)^2+\left(\frac{l}{a_\perp}\right)^2=\left(\frac{2\sin\theta_{epi}}{\lambda}\right)^2 \tag{2}$$

where a_s is the lattice constant for the substrate, θ_s and θ_{epi} are the angles for the diffraction peaks of the substrates and the ZnTe epilayers, respectively, and h, k and l are the Miller indices of the diffraction planes.

The lattice constants measured for ZnTe grown on various substrates are summarized in Table 2. Compared with the reported lattice constant of bulk ZnTe at room temperature (6.1037 Å) [9], the $a_\perp$ lattice parameters of all ZnTe epilayers are smaller, which indicates residual tensile strain (parallel to the surface). The major factors related to this residual tensile strain are the lattice constants, thermal expansion coefficients, and growth temperatures. The lattice constants and thermal expansion coefficients for bulk GaAs, InP, InAs, GaSb and ZnTe are listed in Table 3 [9]. ZnTe has a larger bulk lattice constant than all of the substrate materials (GaAs, InP, InAs and GaSb) used in this study. Therefore, compressive strain due to this lattice mismatch is induced during the initial ZnTe growth at the growth temperature. Such compressive strain can be easily measured when the ZnTe layer is thin (~110 nm), as reported in our previous study [2]. However, when the ZnTe layers are grown beyond a certain critical thickness, the strain due to the lattice mismatch between ZnTe and the specific substrate becomes fully relaxed at the growth temperature. For example, it has been reported that the critical thickness for ZnTe grown on GaAs (0 0 1) substrate by MBE is about 15 nm, compared with 180 nm for ZnTe grown on GaSb substrate using organometallic vapor phase epitaxy (OMVPE) [10,11]. Therefore, for ZnTe thicknesses in the range of 2.3–2.5 μm, it is reasonable to assume that the compressive strain due to lattice mismatch is fully relaxed in the ZnTe epilayers at the growth temperature. Moreover, ZnTe has a larger thermal expansion coefficient ($8.33\times10^{-6}\,K^{-1}$) than that of all of the substrate materials. Thus, when the samples are cooled down to room temperature after the growth, the thermal shrinkage of the ZnTe epilayers is greater than for the substrates. Accordingly, tensile strain occurs in the ZnTe epilayer.

The misfit dislocations present at the various ZnTe/substrate interfaces are studied using HREM. As visible in Fig. 3(a), low magnification images of the ZnTe/GaAs sample show a high density of misfit dislocations near the interface, which is attributed to the large lattice mismatch of 7.3% between ZnTe and GaAs. It is also apparent that the dislocation density becomes much less as the

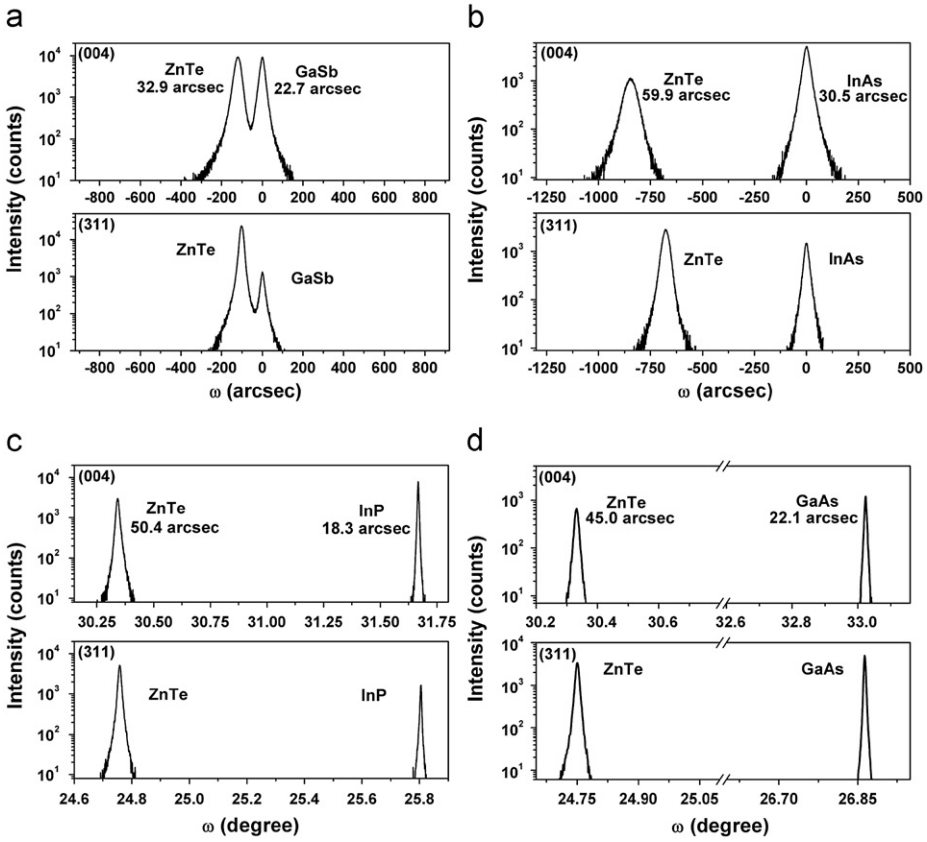

Fig. 2. XRD ω–2θ rocking curves measured in the vicinity of the (0 0 4) and (3 1 1) diffraction peaks for ZnTe growth on: (a) GaSb (0 0 1) substrate; (b) InAs (0 0 1) substrate; (c) InP (0 0 1) substrate and (d) GaAs (0 0 1) substrate.

Table 2
Measured lattice parameters of the ZnTe epilayers grown on different substrates.

Sample no.	$a_{\perp}$ (Å)	$a_{\parallel}$ (Å)
I (ZnTe/GaAs)	6.1014	6.1046
II (ZnTe/InP)	6.0995	6.1052
III (ZnTe/InAs)	6.1016	6.1045
IV (ZnTe/GaSb)	6.1014	6.1042

Table 3
Lattice constant and thermal expansion coefficients of bulk materials [9].

Bulk material	Lattice constant (Å)	Thermal expansion coefficient ($1\times10^{-6}\,K^{-1}$)
GaAs	5.654	5.75
InP	5.869	4.56
InAs	6.059	5.00
GaSb	6.096	6.35
ZnTe	6.104	8.33

ZnTe thickness increases. The high magnification image in Fig. 3(b) shows that there are pseudo-periodic dislocations present at the ZnTe/GaAs interface. Burgers' circuits drawn directly on high magnification images indicate that ~39% of these dislocations are Lomer edge dislocations, with the remainder being 60° partial dislocations. As shown in Fig. 3(c), the Burgers vector of the Lomer dislocation labeled with an arrow corresponds to one-half lattice spacing along the [1 1 0] direction, i.e. $a_0/2$ [1 1 0].

PL measurements are carried out to study the optical properties of the ZnTe samples. The PL spectra of all the ZnTe samples measured at 300 K are shown in Fig. 4(a). Regardless of the substrates, all the PL peaks are at 2.26 eV. The PL emission from ZnTe epilayer grown on GaSb has the strongest intensity, which is attributed to the minimal defect density in the epilayer due to the smallest lattice mismatch of 0.13% between ZnTe and GaSb. Similarly, the sample of ZnTe grown on InAs with a lattice mismatch of 0.75% shows much stronger PL intensity than that of the other two ZnTe samples grown on InP and GaAs substrates, which have larger lattice mismatches of 3.85% and 7.30%, respectively. Temperature-dependent PL spectra of ZnTe grown on GaAs are shown in Fig. 4(b). As temperature increases, the PL peak shows red-shift due to decrease in the bandgap energy, and the FWHM of the PL spectrum becomes broader as expected. In addition, a broad PL emission below bandgap energy is observed at 80 K. This emission is attributed to defects related optical transitions, and more detailed study will be published separately.

4. Summary

The use of thick epitaxial grown ZnTe as a low-cost virtual substrate is proposed for various device applications and high-quality thick ZnTe layers are successfully grown on various GaAs, InP, InAs and GaSb (0 0 1) substrates using MBE. High-resolution XRD results show narrow FWHM (33–60 arcsec) for the ZnTe epilayers grown on all four different substrates. The lattice parameters for ZnTe epilayers along the growth direction ($a_{\perp}$) and in the layer plane ($a_{\parallel}$) are measured and show that residual tensile strains are present in the ZnTe layers due to the difference in thermal expansion coefficients between the epilayers and the substrates. HREM images reveal that Lomer edge dislocations and 60° partial

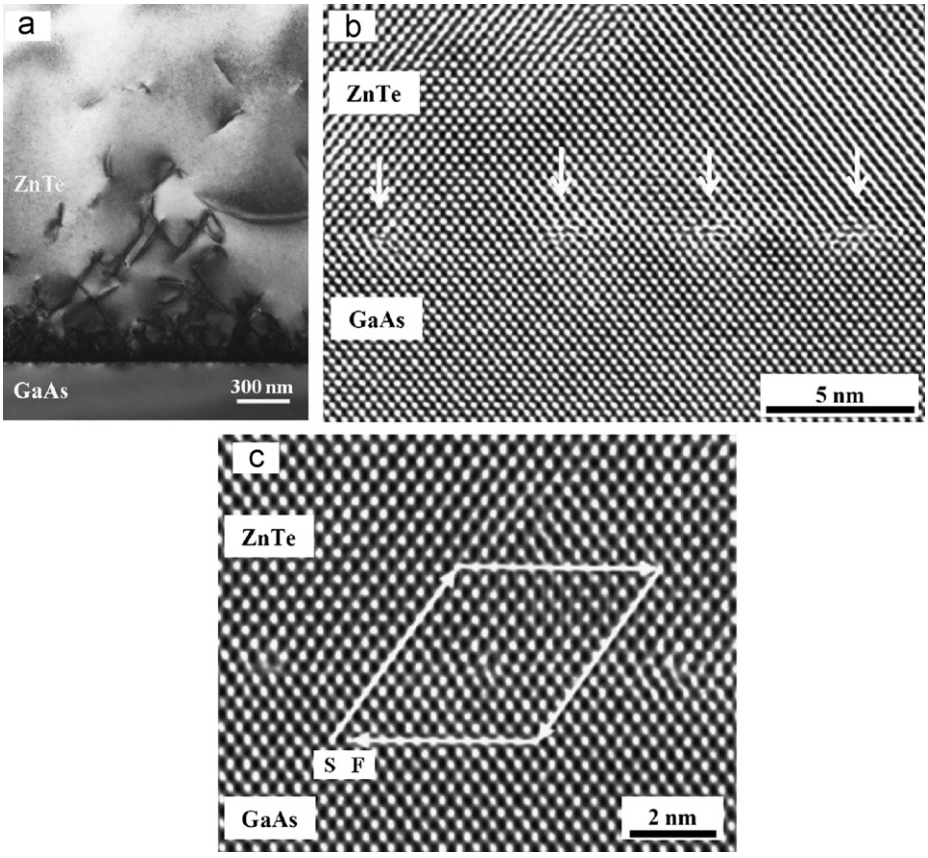

Fig. 3. (a) Low magnification HREM image of ZnTe/GaAs (0 0 1) sample. (b) High magnification HREM image. (c) High-resolution image showing ZnTe/GaAs interface with Burgers' circuit. S and F indicate the start and finish points for the Burgers' circuit analysis.

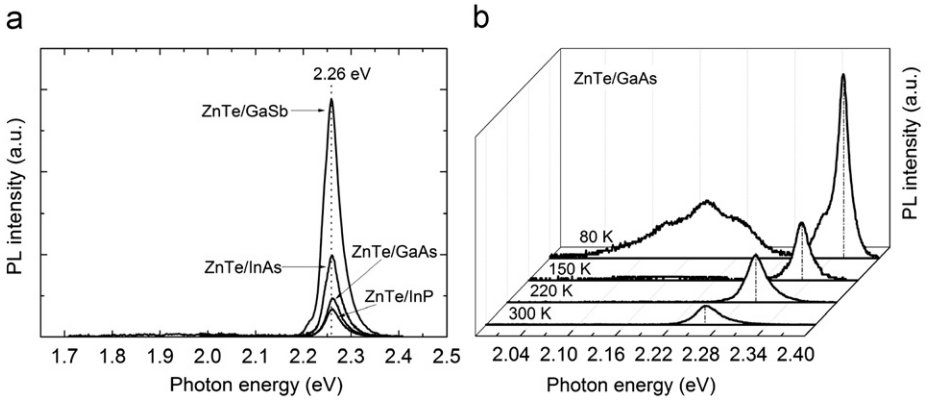

Fig. 4. (a) PL spectra of all the ZnTe samples measured at 300 K. (b) Temperature-dependent PL spectra of ZnTe/GaAs sample.

dislocations are the predominant defects present at the ZnTe/GaAs and ZnTe/InP interfaces. The defect densities in all films become lower as the ZnTe thickness is increased. Strong PL spectra for all the ZnTe samples are observed from 80 to 300 K. The PL peak positions of ZnTe epilayers are at 2.26 eV at room temperature.

Acknowledgments

The authors gratefully acknowledge the use of facilities in the John M. Cowley Center for High Resolution Electron Microscopy, the Center for Solid State Electronics Research, and the LeRoy Eyring Center for Solid State Science at Arizona State University. The work at ASU is partially supported by Science Foundation Arizona, contracts SRG 0190-07 and SRG 0339-08, and by the Air Force Research Laboratory/Space Vehicles Directorate, Contract FA9453-08-2-0228, and AFOSR Grant FA9550-10-1-0129. The work at Notre Dame is partially supported by an NSF program, contract ECCS-1002072, and the same Air Force Research Laboratory/Space Vehicles Directorate program.

References

[1] Y.-H. Zhang, S.-Q. Yu, S.R. Johnson, D. Ding, S.-N. Wu, in: Proceedings of the 33rd IEEE Photovoltaic Energy Specialist Conference, 2008, p. 20.
[2] S. Wang, D. Ding, X. Liu, X.-B. Zhang, D.J. Smith, J.K. Furdyna, Y.-H. Zhang, J. Cryst. Growth 311 (2009) 2116.

[3] K. Sato, M. Hanafusa, A. Noda, A. Arakawa, M. Uchida, T. Asahi, O. Oda, J. Cryst. Growth 214 (2000) 1080.
[4] J.H. Chang, T. Takai, K. Godo, J.S. Song, B.H. Koo, T. Hanada, T. Yao, Phys. Status Solidi B 229 (2002) 995.
[5] A. Million, N.K. Dhar, J.H. Dinan, J. Cryst. Growth 159 (1996) 76.
[6] N.K. Dhar, C.E.C. Wood, A. Gray, H.Y. Wel, L. Salamanca-Riba, J.H. Dinan, J. Vac. Sci. Technol. B 14 (1996) 1.
[7] S. Rujirawat, L.A. Almeida, Y.P. Chen, S. Sivananthan, D.J. Smith, Appl. Phys. Lett. 71 (1997) 1810.
[8] S. Adachi, Handbook on Physical Properties of Semiconductors. Volume 2: III–V Compound Semiconductors, Kluwer, Boston, 2004.
[9] S. Adachi, Properties of Group-IV III–V and II–VI Semiconductor, Wiley, West Sussex, England, 2005.
[10] V.H. Etgens, M. Sauvage-Simkin, R. Pinchaux, J. Massies, N. Jedrecy, A. Waldhauer, S. Tatarenko, P.H. Jouneau, Phys. Rev. B 47 (1993) 16.
[11] P. Tomasini, A. Haidoux, M. Maurin, J.C. Tedenac, J. Cryst. Growth 166 (1996) 590.